Developments in Environmental Science, volume 2, pp. 299–324
ISSN: 1474-8177

Chapter 13

Formulation and application of regional air quality modeling for integrated assessments of urban and wildland pollution

Gail Tonnesen, Zion Wang, Mohammad Omary, and Chao-Jung Chien

Center for Environmental Research and Technology, Bourns College of Engineering, University of California, Riverside, CA 92521, USA
E-mail: tonnesen@mail.cert.ucr.edu (G. Tonnesen), wang@mail.cert.ucr.edu (Z. Wang), omary@cert.ucr.edu (M. Omary).

Abstract

Anthropogenic emissions into the atmosphere of gaseous pollutants such as nitrogen oxides (NO_x) and volatile organic compounds (VOC) produce secondary atmospheric pollutants, including ozone (O_3), nitric acid (HNO_3), and aerosol nitrates (NO_3) that may have adverse effects on wildland ecosystems. It is difficult to quantify the sources and magnitude of the deposition fluxes of these species using ambient monitoring studies because field measurements are expensive and typically have poor spatial coverage. Moreover, ambient monitoring is not well suited for determining the sources and transport of pollutants nor for identifying optimal control strategies to reduce pollutant exposure. Complex chemistry-transport models have been widely used for short-term modeling of urban and regional air quality and have been used for long-term modeling of acid deposition in the eastern US. We report results of annual model simulations in the western US designed specifically to study regional haze and including predictions of deposition of O_3 and nitrogen (N) species in the Sierra Nevada. The modeling system used is the US Environmental Protection Agency's (USEPA) Community Multiscale Air Quality (CMAQ) model, which was developed in the "third generation" (Models-3) modeling system that supersedes earlier generation models such as the Regional Acid Deposition Model. The development of emissions inventories, meteorological fields, and the ambient data necessary for model performance evaluation is a large-scale, complex effort that involves multiple institutions and years of effort. We describe the model formulation and the necessary data sets, and we provide some sample results of deposition of O_3 and N in the Sierra Nevada. There are large uncertainties in the deposition fluxes estimated in this modeling study, and considerable further work is required to develop more accurate input data. Moreover, the current study used a relatively poor spatial resolution with a grid cell dimension of 36 km. Finer resolution modeling will be required to simulate more confidently the wind fields and the spatial variability of deposition fluxes in the Sierra Nevada.

1. Introduction

Awareness of urban air quality and concern for its possible health effects extends at least back to the 12th century, when the philosopher Moses Maimonides wrote: "Comparing the air of cities to the air of deserts and arid lands is like comparing waters that are befouled and turbid to waters that are fine and pure" (Finlayson-Pitts and Pitts, 1986, p. 3). The degradation of urban air quality accelerated during the industrial revolution and culminated in extreme air pollution events during the 1950s in which thousands of fatalities were attributed to urban smog (Wilkins, 1954). In the US, this prompted the formation of local, state, and federal agencies to oversee the protection of urban air quality and the adoption by the federal government of the Clean Air Act of 1965. The Clean Air Act (CAA) established National Ambient Air Quality Standards (NAAQS) for a variety of urban air pollutants including ozone (O_3), sulfur dioxide (SO_2), nitrogen dioxide (NO_2), carbon monoxide (CO), lead, and total suspended particulate (TSP) matter. After epidemiological studies showed a strong correlation between increased mortality and levels of fine particle matter (PM), new air quality standards were implemented for fine particulate matter with diameter of less than 10 microns (PM10) and less than 2.5 microns (PM2.5) (USEPA, 1997a). In addition to its health effects, PM2.5 also absorbs and scatters light causing the familiar urban haze.

Beginning in the early 1980s, it became widely recognized that the effects of urban and industrial air pollution extended beyond the cities to the deserts, arid lands, and other ecosystems that previously had been "fine and pure." As a result, subsequent amendments to the CAA in 1990 expanded the scope of regulatory activities to address regional scale air pollution problems such as acid deposition (NAPAP, 1991), regional O_3 (National Research Council, 1992), and regional haze that obscures scenic vistas in the national parks and forests (National Research Council, 1993). Recent research has also focused on atmospheric nitrogen (N) deposition and its role in eutrophication of surface waters (Vitousek et al., 1997; USEPA, 1997b; Valigura et al., 2001).

Although urban air pollution is known to affect pristine areas, there remains considerable uncertainty about the transport and fate of urban air pollutants and about the relative blame for urban versus local sources in contributing to air pollutants in pristine areas. This uncertainty arises in part because of the uncertainty in photochemical reactions and because of the complex interaction of emissions, chemistry and meteorological processes. For the case of O_3 production, there is additional uncertainty because of the complex, non-linear dependence of O_3 formation on its precursor species, volatile organic compounds

(VOC) and nitrogen oxides (NO_x). Moreover, there is uncertainty in the contribution of biogenic VOC emissions to O_3 formation, and it is difficult to fully characterize the transport and interaction of biogenic VOC with anthropogenic VOC and NO_x emissions.

Air quality models have been developed to characterize and study the processes affecting air pollutants (Russell and Dennis, 2000). These air quality models have been widely used to study urban air pollution for episodic conditions of a few days or weeks and for developing emissions control strategies for the NAAQS pollutants. There have been a few applications using simplified air quality models applied for long-term continental domains; for example, the Regulatory Modeling System for Aerosols and Deposition (REMSAD) is a simplified model that was developed to study aerosol species and regional haze (ICF, 2002). However, there has been very limited application of advanced air quality models for studying the long-term budgets of O_3, PM, and nitrogen for the national parks and forests. This limitation is due largely to the high cost of developing the necessary emissions inventories and meteorological data and the high computational cost of performing long-term air quality model simulations. Nonetheless, it is recognized that long-term modeling using sophisticated air quality models is needed to analyze the budgets of O_3, N, and PM, and their effects on wildlands.

Through a multi-institutional effort funded by the USEPA and the Western Governors' Association, we are currently carrying out a major air quality modeling study for the Class I areas in the western US. Class I areas are defined to include national parks and forests with areas greater than 5000 acres. The motivation of this study is an assessment of regional haze; however, to simulate regional haze the model must adequately simulate photochemistry (O_3) and inorganic aerosol physics and chemistry and secondary organic aerosol production. The model simulations have been run for calendar year 1996 allowing us to characterize seasonal budgets of O_3, N, and PM in the Sierra Nevada. The model simulations were evaluated by comparison with ambient monitoring data for O_3 by using the Aerometric Information Retrieval System (AIRS) and for PM using the Interagency Monitoring of Protected Visual Environments (IMPROVE) monitoring sites (Malm, 2000). (Results from the model performance evaluation are available at the Web site http://pah.cert.ucr.edu/rmc.) This chapter outlines the emissions, meteorological, and chemical processes that affect regional scale air pollutants, and it summarizes recent developments in air quality research that attempt to provide integrated assessments for pollutants affecting wildlands. Results of our large-scale regional haze modeling study are presented to illustrate the distribution of O_3 and N deposition in the Sierra Nevada.

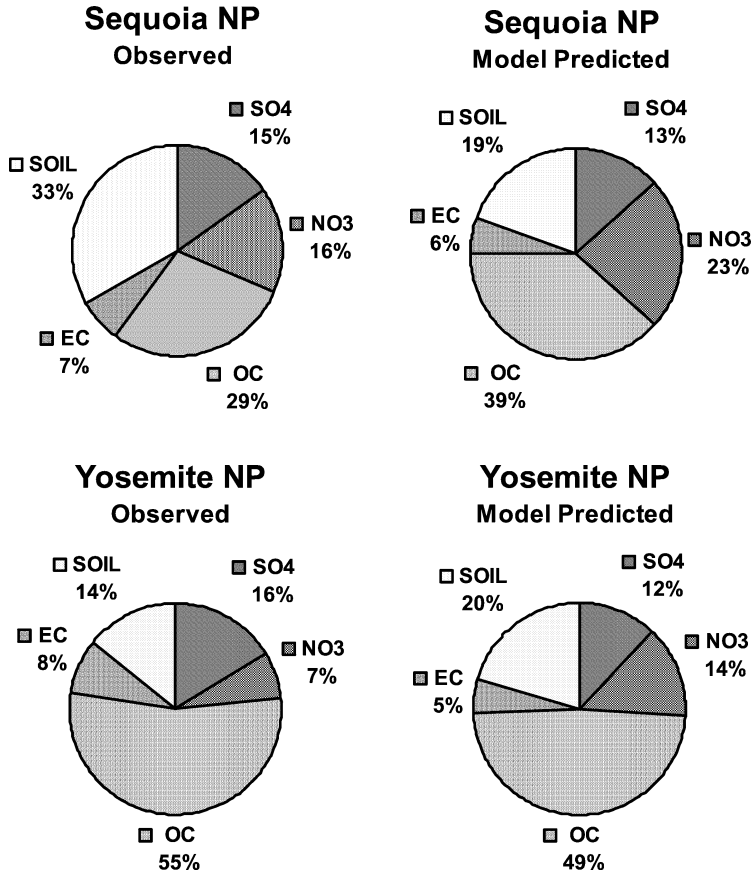

Figure 1. Relative contribution of SO_4^{2-}, NO_3^-, organic carbon (OC), elemental carbon (EC) and soil to fine particulates at Sequoia National Park (top) and at Yosemite National Park (bottom). The left panel shows average of ambient observations during the summer of 1996, and the right panel shows model predictions for the same period.

2. Chemistry of air pollutant formation

Many of the key air pollutants of interest for wildlands including O_3, ammonium sulfates, ammonium nitrate, and secondary organic aerosols (SOA) are secondary products that are formed through photochemical reactions of their precursor species VOC, NO_x, and ammonia (NH_3). Ambient monitoring data for these secondary PM species are typically measured and reported as total nitrate (NO_3^-), sulfate (SO_4^{2-}) and ammonium ion (NH_4^+) and as organic mass. Our current research is focused on the PM species that contribute to regional

haze in Class I areas. There is some regional variability in the contribution of primary and secondary pollutants to fine PM among the nation's Class I areas. In the eastern US ammonium sulfates represent a major fraction of fine PM, while in the arid southwestern US crustal materials tend to be a large contributor. For the Sierra Nevada, SOA is the single largest contributor to fine PM (Malm, 2000). Fig. 1 shows annual average percentage contributions of SOA (organic carbon), nitrate, sulfate, crustal materials and elemental carbon for Sequoia and Yosemite National Parks both for ambient data and model predictions. Although nitrate represents less than half of the total fine PM, it is of special interest because nitrate deposition is a source of biologically active nitrogen that can affect forested ecosystems or, through surface runoff, can cause eutrophication of surface waters. Although O_3 does not play a direct role in light extinction or visibility, it is an important pollutant in its own right and its photochemistry plays a critical role in the secondary photochemical production of nitrates, sulfates, and SOA (Gao et al., 2001). Moreover, deposition of O_3, HNO_3, and other secondary pollutants to leaf surfaces can cause direct damage to forests (e.g., Reich and Amundson, 1985; USEPA, 1996; Bytnerowicz et al., 1999).

2.1. Gas phase photochemistry

Production of O_3 in the troposphere occurs almost exclusively by photochemical reactions of VOC and NO_x. Urban or urban influenced air masses typically have relatively high concentrations of both VOC and NO_x and exist in a chemical regime where NO_x and free radicals ($HO_x = OH + HO_2 + RO_2$) catalyze the production of oxidants, including O_3, NO_2, and peroxyacylnitrates (PAN). Thus, the production of O_3 and other secondary pollutants requires a source of free radical production, and this is believed to occur primarily by photolysis reactions as shown in reactions 1 through 4:

$$HCHO + h\nu \rightarrow 2\,HO_2 + CO \tag{R.1}$$

$$HO_2 + NO \rightarrow OH + NO_2 \tag{R.2}$$

and

$$O_3 + h\nu \rightarrow \dot{O}_1 + O_2 \tag{R.3}$$

$$\dot{O}_1 + H_2O \rightarrow 2\,OH \tag{R.4}$$

The hydroxyl radical (OH) can then attack VOC to produce O_3 as shown by reactions (R.5)–(R.12) using methane as an example to illustrate typical VOC chemistry:

$$OH + CH_4 \rightarrow H_2O + CH_3O_2 \tag{R.5}$$

$$CH_3 + O_2 \rightarrow CH_3O_2 \quad \text{(R.6)}$$

$$CH_3O_2 + NO \rightarrow CH_3O + NO_2 \quad \text{(R.7)}$$

$$CH_3O + O_2 \rightarrow HCHO + HO_2 \quad \text{(R.8)}$$

$$HO_2 + NO \rightarrow NO_2 + OH \quad \text{(R.9)}$$

$$2x\,NO_2 + h\nu \rightarrow NO + O(^3P) \quad \text{(R.10)}$$

$$2x\,O(^3P) + O_2 \rightarrow O_3 \quad \text{(R.11)}$$

Net reaction: $CH_4 + 4\,O_2 \rightarrow 2\,O_3 + HCHO + H_2O$ (R.12)

Reaction (R.12) is the net reaction from summing (R.5)–(R.11) and shows that this is a catalytic process in which neither the radical nor the NO_x is destroyed. However, there are other reactions that terminate the free radicals or that convert reactive NO_x to inert forms of odd nitrogen defined as $NO_z = HNO_3 + RNO_3 + PAN$. A single molecule of OH typically contributes to the production of several molecules of O_3 before the radical is destroyed in a radical termination reaction. For urban influenced conditions with high NO_x concentrations, radical termination occurs primarily by reaction of OH with NO_2 and reaction of organic peroxy radicals with NO_x:

$$OH + NO_2 \rightarrow HNO_3 \quad \text{(R.13)}$$

$$RO_2 + NO \rightarrow RNO_3 \quad \text{(R.14)}$$

$$RO_3 + NO_2 \rightarrow PAN \quad \text{(R.15)}$$

For rural or remote environments with low NO_x, radical termination occurs primarily by peroxy radical self-reactions that produce hydrogen peroxide (H_2O_2) and organic peroxides (ROOH):

$$HO_2 + HO_2 \rightarrow H_2O_2 + O_2 \quad \text{(R.16)}$$

$$HO_2 + RO_2 \rightarrow ROOH + O_2 \quad \text{(R.17)}$$

The number of O_3 molecules produced per molecule of NO_x varies greatly depending on the ratio of VOC to NO_x. For daytime photochemistry (R.13)–(R.15) are major pathways that convert reactive NO_x to NO_z. There is also nighttime chemistry that converts NO_x to NO_z as follows:

$$NO_2 + O_3 \rightarrow NO_3 + O_2 \quad \text{(R.18)}$$

$$NO_3 + NO_2 \rightarrow N_2O_5 \quad \text{(R.19)}$$

$$N_2O_5 + H_2O \rightarrow 2\,HNO_3 \quad \text{(R.20)}$$

A single molecule of NO_x typically contributes to just a few O_3 for very high NO_x conditions in which (R.13) and (R.20) are dominant. For example, emissions of NO_x from power plants have very low VOC/NO_x ratios and may produce as few as 1 or 2 molecules of O_3 per NO_x, and urban plumes with high NO_x concentrations may produce on the order of less than 10 molecules of O_3 per NO_x (Daum et al., 2000; Kleinman et al., 2000).

For typical rural or remote conditions where NO_x concentrations are very low, the current modeling study shows that a molecule of NO_x can contribute to production on the order of 10 to 100 molecules of O_3 before being converted to inert NO_z. A large portion of the rural VOC is from biogenic emissions, and this contributes to the high VOC/NO_x ratios and consequent high production efficiency of O_3 per NO_x in rural and remote atmospheres (Pierce et al., 1998).

Therefore, for typical urban conditions of high NO_x emissions and low VOC/NO_x ratios, OH reacts preferentially with NO_2 to destroy the OH radical. For these conditions, reducing VOC emissions is the most effective strategy for reducing O_3 because this limits the radical propagation reactions of OH with VOC (e.g., (R.5)). Moreover, for urban conditions, reductions in NO_x emissions can cause increases in urban O_3 levels by reducing the NO_2 reaction with OH and increasing ambient OH levels (Tonnesen and Jeffries, 1994). (More comprehensive reviews of gas phase chemistry are provided by Kleinman (1994), Jeffries and Tonnesen (1994), Sillman (1995), Atkinson (2000), and Dodge (2000).)

2.2. Aerosol formation and dynamics

The treatment of aerosols in air quality models (AQMs) introduces another level of complexity beyond that of gas chemistry because the properties and fate of aerosols depend strongly on the aerosol size distribution. Aerosols can be classified according to size distributions where fine particulates are defined as those having an aerodynamic diameter of less than 2.5×10^{-6} meters, or microns (μm), and coarse particulates are defined to have diameter greater than 2.5 μm. Fine particulates are further classified as either Aitken mode (size range from 0.010 to 0.100 μm) or accumulation mode (size range from 0.100 to 2.5 μm). Aitken mode particulates are formed by nucleation or condensation of gas phase species, e.g., nucleation through the equilibrium relationship: $NH_4NO_3(s) \Leftrightarrow NH_3(g) + HNO_3(g)$. Accumulation mode particulates are formed by coagulation of finer particles or by condensation on existing particulates. In addition to the size distribution, the number distribution and mass distribution of aerosols also affects their chemical and optical properties as well as the dynamic interactions among aerosols and between aerosols and gas phase species.

Two approaches have been employed to represent the number, size and mass distributions of particulates. In a *sectional* approach the aerosol species are represented by using several discrete size bins. To achieve greater levels of accuracy, the sectional method must use increasing numbers of size bins. Moreover, the size distribution must be represented separately for each aerosol species; therefore, the computational cost of sectional approaches can become prohibitively expensive if large numbers of bins and aerosol species are represented in the model. An alternative method is a *modal* approach in which the number, size, and mass distributions are represented as a superposition of lognormal distributions called modes (Whitby, 1978). The modal approach is employed in the version of the USEPA's Models-3 Community Multiscale Air Quality (CMAQ) model used in the present study, and it uses three different size distributions: the Aitken mode, the accumulation mode, and the coarse mode (Binkowski, 1999).

The deposition velocity and the atmospheric lifetime of N species varies considerably depending on the partitioning of N among gas phase and aerosol species (McRae and Russell, 1984). The rate of N deposition increases as NO is converted first to NO_2, and then to HNO_3, and the deposition velocity of HNO_3 is greater than that of NO_3^-. Thus, to estimate the transport and fate of N, it is necessary to simulate both gas phase and heterogeneous production of HNO_3, and the model must also treat the partitioning of HNO_3 between the gas and aerosol phase NO_3^- by using a thermodynamics model of H_2SO_4, HNO_3, and NH_3.

Chemical pathways that lead to aerosol nitrate production are summarized in Fig. 2. NO_x emissions occur primarily as NO in urban areas and are converted first to NO_2 and then to HNO_3 in gas phase photochemistry. HNO_3 formed by gas phase oxidation of NO_2 is very soluble in water and is the principal source of nitrate in precipitation. The reaction of HNO_3 and NH_3 to form ammonium nitrate (NH_4NO_3) is also a major pathway to form particulate nitrate.

HNO_3 also reacts with coarse mode sea salt aerosols (NaCl) to form coarse mode sodium nitrate:

$$HNO_3(g) + NaCl(s) \rightarrow NaNO_3(s) + HCl(g) \qquad \text{(R.21)}$$

The formation of coarse aerosols from sea salt displacement reactions can enhance the rate of dry nitrate deposition, particularly in coastal areas. During nighttime the reaction of N_2O_5 with NaCl (the major component of sea salt) has also been shown to lead to $NaNO_3$, providing another source of nitrate aerosol in the coastal region (Finlayson-Pitts and Pitts, 1986). The NO_3 radical formed also reacts with a series of organic compounds, producing organic nitrates.

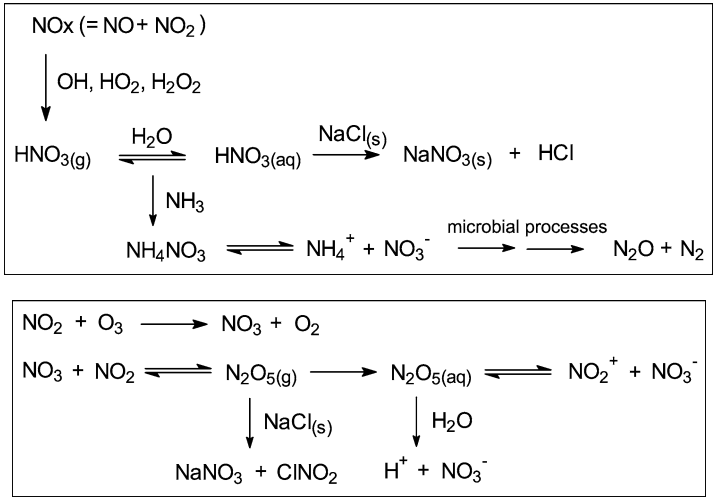

Figure 2. Chemical pathways for nitrate production and transformation (top); and nighttime formation of nitrate (bottom).

Sources of secondary organic aerosols include reactions of both anthropogenic VOC (e.g., Kleindienst et al., 1999) and biogenic VOC (Kavouras et al., 1999) and have seasonal variability (Strader et al., 1999).

Because of the complexity and variability of the processes—both homogeneous and heterogeneous reactions—it is essential to understand the evolution of both gaseous and aerosol species that involve nitrate particular matter. Thus, to be able to predict or simulate the fate of nitrate particulates, an aerosol model is needed that accounts for physico-chemical processes, including gas-phase chemistry, aqueous chemistry, condensation, adsorption, partition, etc. Comprehensive reviews of aerosol dynamics and chemistry are provided by Seinfeld and Pandis (1998), and modeling of aerosol formation in California has been reviewed by Hughes et al. (1999) and Christoforou et al. (2000).

2.3. Estimates of dry and wet deposition

Dry and wet and deposition of aerosol species and gas phase species (including O_3, SO_2, HNO_3, NO, NO_2, PAN, NH_3, H_2O_2, organic peroxides, and aldehydes) are represented in the CMAQ model (Binkowski, 1999). Dry deposition is calculated as the product of species concentrations at the surface and a dry deposition velocity (v_d). The method of Wesley (1989) is used to calculate v_d

for the gas phase species:

$$v_d = \frac{1}{R_a + R_b + R_c} \quad (1)$$

In Eq. (1) R_a represents aerodynamic resistance and is determined from estimates of turbulence in the surface layer using meteorological data or models. R_b represents the quasi-laminar boundary layer resistance and is calculated using the species molecular diffusivity and the surface friction velocity, which varies with land use type. R_c represents the canopy resistance and is determined from ambient measurements for O_3 and SO_2 as a function of season, insolation, surface wetness, and land type. However, because there are insufficient measurements for other species, the value of R_c is qualitatively scaled to the values of O_3 and SO_2. For dry deposition of aerosol species the deposition velocity is calculated as the sum of the aerodynamic resistance term and a gravitational settling velocity (Binkowski and Shankar, 1995).

Wet deposition of gas and aerosol species is treated in the CMAQ cloud dynamics scheme, which represents convective transport, aqueous chemistry, mass transfer to the aqueous phase, and rainout (Roselle and Binkowski, 1999). The cloud treatment includes parameterizations for several different types of clouds, including sub-grid scale convective, grid scale resolved clouds, and precipitating and non-precipitating clouds (Dennis et al., 1993). Cloud water fractions and precipitation rates are calculated in the meteorological model and passed to the CMAQ model through the meteorological preprocessor. Transfer of gas phase species to the aqueous phase is determined using cloud water fractions, Henry's Law constants, dissociation constants, and cloud water pH. Coarse aerosols with diameter greater than about 2.5 μm are assumed to be immediately absorbed by cloud water for grid cells containing clouds. Absorption into cloud droplets of Aitken mode aerosols is treated using a model of mass transfer in the interstitial cloud space (Binkowski and Shankar, 1995).

New deposition schemes are under development for the CMAQ model that will provide a more sophisticated treatment of dry deposition by taking into account plant physiology. For example, plant uptake gas species responds to soil moisture, heat and water stress, and feedback on plant stomata. The direct plant uptake can be modeled to estimate the true exposure or dose. This approach will be more accurate than the current scheme, which only represents a total dry deposition flux as a surface boundary condition.

3. Methods and models used

An air quality modeling system is composed of a variety of numerical models and datasets that represent emissions inventories, meteorology, and chemistry.

3.1. Chemistry-transport models

Numerical simulation models have been widely used since the 1970s for managing urban air pollution (e.g., Russell and Dennis, 2000; National Research Council, 1992). These models are typically referred to as chemical transport models (CTMs) or air quality models (AQMs), and they are used to characterize the atmospheric budgets of important trace species including O_3, PM, and a wide variety of toxic air pollutants. Formally, the model is a system of partial differential equations (PDEs) that represent the conservation of mass for each trace species represented in the model:

$$\frac{\partial C_i}{\partial t} + \nabla \cdot \mathbf{V} C_i = -\nabla \cdot \mathbf{D} \nabla C_i + P_i(\mathbf{C}) - L_i(\mathbf{C}) C_i + S_i \quad \text{for } i = 1, \ldots, n \tag{2}$$

where n is the number of species represented in the photochemical mechanism, and C_i represents the trace species concentration. Other terms in Eq. (2) include the chemical production rate (P_i) and loss frequency (L_i), transport by advective processes ($\mathbf{V}C_i$) where $\mathbf{V}$ represents the wind vector, and dispersion from small and large scale eddies in the atmosphere where $\mathbf{D}$ represents the turbulent dispersion coefficient. Species concentrations may also be affected by other sink and source terms (S) such as emissions and deposition. Eq. (2) produces a system of n non-linear PDEs that are coupled by $\mathbf{C}$, which is the species concentration vector ($\mathbf{C} = [C_1 + C_2 + \cdots + C_n]$). Eq. (2) cannot be solved analytically, but various numerical methods can be used to obtain accurate solutions, and these are typically encoded as large FORTRAN programs (e.g., McRae et al., 1982).

The numerical methods used in solving Eq. (2) can be divided into two main categories: Lagrangian approaches and Eulerian approaches. Lagrangian models are often referred to as trajectory models because they simulate photochemistry in parcels of air that follow the wind trajectory. The frame of reference is defined relative to the wind vector, and the advection term drops out of Eq. (2). If turbulent dispersion is also ignored, Eq. (2) reduces to a system of ordinary differential equations (ODE):

$$\frac{dC_i}{dt} = P_i(\mathbf{C}) - L(\mathbf{C}) C_i + S_i \quad \text{for } i = 1, \ldots, N \tag{3}$$

and the problem reduces to the solution of a system of ODEs. Trajectory models with multiple air parcels have been widely used to study transport and deposition of pollutants in Europe (Simpson, 1992). However, it is difficult to represent the interaction and mass transfer among parcels in a trajectory model, and trajectory models can become computationally expensive for fine resolution modeling, which requires the use of a large number of air parcels.

For these reasons, beginning in the late 1980s, air quality modelers in the US have primarily used gridded, Eulerian models.

Eulerian approaches divide the problem domain into a grid of discrete elements or cells. The first Eulerian AQMs were limited to the urban scale and used grid resolutions on the order of 4 km. The realization that long-range transport of pollutants and their precursors can impact local control strategies and the need to study regional impacts (as well as rapidly increasing computational resources) led to the use of coarse-grid regional scale models (e.g., RADM; Chang et al., 1987) to define the boundary conditions for urban scale AQMs such as the Regional Oxidant Model (ROM; Lamb, 1983). More recently, multi-scale models have been developed that nest several levels of increasingly refined grids within a single modeling system; examples include the CAMx model (ENVIRON, 1998) and the CMAQ model (Byun and Ching, 1999). This approach is still impractical to adequately resolve the fine scale structure in species distributions caused by intense point source emissions. Fine scale resolution of point source plumes has been achieved using nested plume-in-grid (PiG) modules (Gillani and Pleim, 1996).

In this study, the AQM used is the CMAQ model (Byun and Ching, 1999), which is a system composed of a suite of models that preprocess the input data including meteorological fields, emissions inventories, initial conditions, and boundary conditions. The preprocessors provide the input for the CMAQ Chemical Tracer Model (CCTM), which is used to simulate the transport, chemical transformations, and fate of the emitted species. In this study the CCTM simulations were performed on a three-dimensional grid that extended from the Pacific Ocean to Illinois and from northern Mexico to southern Canada. The grid was defined using a 36 km resolution grid with 95×85 grid cells in each layer and 18 vertical layers extending from the ground to about 18,000 meters above sea level.

The CMAQ systems allow for a variety of choices for treating the numerical solution of the transport processes and chemistry (Byun and Ching, 1999). In this study we selected the piecewise parabolic method (Colela and Woodward, 1984) for solving advective transport. We used the Carbon Bond IV (CB4) condensed photochemical mechanism (Gery et al., 1989) to represent the gas phase photochemistry, and we used a modified Eulerian backward implicit method to solve the photochemistry (Hertel et al., 1993). The most recent version of the CMAQ aerosol chemistry (AE2; Binkowski, 1999) was used to couple the gas phase and aerosol chemistry.

3.2. Emissions modeling

Inventories of pollutant emissions are the key input data for AQMs, and they are the input data for which the uncertainty is the largest. Inventories must be

prepared for several species including VOC, NO_x, SO_x, CO, NH_3, and primary PM emissions. There are a wide variety of emissions sources, and they are generally classified as the following five categories:

1. Point sources—Primarily large industrial facilities or power plants, for which Continuous Emissions Monitoring (CEMs) data are available or estimated from local, county, or states agencies. Source location is specified as latitude and longitude for each facility, and stack characteristics and meteorological data are needed to estimate the plume rise height.
2. Area sources—Generally small sources from a variety of commercial and consumer activities, such as consumer solvent use, gas stations, agriculture, etc. Spatial allocation of area source emissions are determined by using surrogate information such as census population data or other surrogate information for particular activities. Off road mobile sources such as agricultural and construction equipment are also treated as an area source.
3. Mobile sources—Personal and commercial vehicles, heavy duty diesel trucks, aircraft, trains, ships. Emissions are calculated from estimates of vehicle miles traveled and vehicle emissions factors. Spatial allocations are determined using road link data or other spatial surrogate data for vehicle locations.
4. Biogenic emissions—These are from natural sources such as plants, soil microbial processes and lightning. Emissions rates are estimated using land use information and emissions factors for particular plant types and are located based on the land use data. Because biogenic emissions are highly sensitive to sunlight and temperature, meteorological data must also be supplied to model biogenic emissions.
5. Smoke emissions—These are from wildfires, prescribed burning, and agricultural burning, where these data must be compiled from observations or permitting information. Because the air quality officials are barred from collecting data on agricultural burning in some western states, accurate smoke emissions can be difficult to obtain.

Compiling emissions inventories is the most expensive and tedious aspect of air quality modeling, and it is the area in which mistakes most frequently are made. Moreover, there are very large uncertainties in the emissions factors for many source categories.

In the present study, we used emissions inventories based on the USEPA National Emissions Inventory (NEI) as a starting point, with many updates based on information from state air pollution agencies. Mobile sources were estimated for California using the California Air Resource Board (CARB) mobile source emissions factor model (EMFAC; CARB, 2000). For all other states the USEPA MOBILE version 6 model was used to estimate mobile sources. Biogenic emissions were estimated using the Biogenic Emissions Inventory

System (BEIS2) (Pierce et al., 1998). Wildfire emissions were estimated using data compiled by the US Department of Agriculture (USDA) Forest Service.

Although this is the most detailed and comprehensive emissions inventory ever prepared for long-term air quality modeling, it is nonetheless missing several important emissions categories, such as agricultural and wildland prescribed burning and wind blown dust, for which adequate data are unavailable. Our inventory does include some emissions data for Canada and Mexico; however, the uncertainties in these data are very large.

The data inputs described above are "raw" emissions inventories. An emissions processing system (EPS) is required to determine the appropriate spatial and temporal allocation of emissions within the grid structure used in the model. The EPS must also correctly combine chemical fingerprints from the raw emissions data (i.e., speciate the emissions) into the model species. For example, the CMAQ CTM employs a condensed photochemical mechanism in which a parameterized representation of surrogate VOC species are used to represent the hundreds of explicit VOC species that are present in ambient air. After the EPS has performed the speciation and spatial and temporal allocation of each emissions category, it must merge the various emissions categories and write them into binary data files in the correct format used by the AQM. Houyoux et al. (2000) have developed the Sparse Matrix Operator Kernel Emissions (SMOKE) processing system to integrate high-performance sparse matrix operations and to provide advanced quality assurance of the emissions processing. Finally, it should be noted that processing of emissions is both computationally expensive and requires large amounts of disk space. For this study the final processed emissions data required 200 gigabyte (GB) of disk space for an annual simulation, and approximately 500 GB of additional disk space was required for intermediate files.

Compilation of the annual emissions inventory is a team effort that involves scientists and staff from many state and federal agencies, from academic communities, and consultants. The refinement of this emissions inventory is expected to be a large-scale effort that will continue for several years.

3.3. Meteorological modeling

The meteorological fields are required to solve atmospheric diffusion equations in Eulerian numerical AQMs. Meteorology encompasses many atmospheric processes that control or strongly influence the evolution of emissions, chemical species, aerosols, and particulate matter (Seaman, 1999). These processes include horizontal and vertical transport, turbulent mixing, convection, water content, and both dry and wet deposition to the surface. Meteorology also significantly affects the sources of biogenic emissions of organic compounds.

Therefore, the accuracy of air quality model simulations are heavily dependent on the quality of the meteorology data (Byun, 1999a, 1999b).

Meteorology fields for AQM simulations can be provided either by diagnostic models or dynamic models with or without four-dimensional data assimilation. Dynamic models analyze observations at surface sites and upper air soundings and provide dynamically consistent meteorological fields. They are easy to operate, but require a large amount of observations to adequately describe the fields. Dynamical models integrate the non-linear hydrodynamic equations of motion in a numerical simulation model to produce gridded fields of variables required by the air quality models. Dynamic models utilizing four-dimensional data assimilation (FDDA) attempt to combine the best features of diagnostic and dynamical approaches by integrating a numerical model in which ambient data are used to "nudge" the solution of the numerical equations toward the observed meteorology fields throughout the integration period (Seaman, 1999).

The principal meteorological fields provided to the AQMs include temperature, pressure, horizontal and vertical wind components, water mixing ratio, liquid water contents, cloud fraction, boundary layer depth, vertical diffusion coefficient, surface heat fluxes (heat, moisture, momentum), and solar actinic fluxes. The meteorology fields are usually provided at hourly intervals for the entire duration of the AQM simulation. Ideally, the chemistry-transport model should be fully coupled to a meteorological modeling system. However, air quality modelers typically run the AQMs many times to understand the effects of emissions control strategies on the pollutants concentrations using a given set of meteorology fields. Therefore, to minimize computational cost, the meteorological model is typically run separately from the AQM, and the meteorology fields are saved to an output file at regular time intervals. Then, the AQM reads from and interpolates the meteorology fields from the file. This interpolation can create problems with mass consistency or mass conservation in the AQM. Thus, the interpolation of the meteorology data and AQM numerics must be carefully designed to minimize mass conservation problems (Byun, 1999a, 1999b).

The dynamic meteorology model selected with the Community Multiscale Air Quality (CMAQ) Model is the Fifth-Generation Pennsylvania State University/National Center for Atmospheric Research (NCAR) Mesoscale Model (MM5) (Grell et al., 1994). The MM5 is a three-dimensional prognostic meteorological model available not only for meteorology studies but also for air quality studies. The MM5 was originally developed in the early 1970s and has undergone many changes to increase and broaden its capabilities. It was used to simulate meteorology at 108-km and 36-km resolutions for calendar year 1996 over the entire continental US and portions of Canada, Mexico, and the Atlantic and Pacific Oceans (Olerud et al., 1999).

The version of MM5 used to simulate the 1996 meteorology is MM5 version 2.12 with modifications to allow the output of vertical exchange coefficient (Kv) for use in AQMs. The domain for MM5 covers the entire US at 108-km and 36-km resolutions, and the western half of the US at 12-km resolution. Some of the physics used in the simulation include one-way nesting; non-hydrostatic dynamics; four-dimensional data assimilation of wind, temperature, and mixing ratio; explicit treatment of moisture; cumulus subgrid cloud parameterization with Anthes–Kuo scheme in the 108-km grid and Kain–Fritsch scheme in the 36-km grid; vertical mixing of momentum in the mixed layer; planetary boundary layer (PBL) parameterization; atmospheric radiation; sea ice treatment; and snow cover. Atmospheric radiation was adjusted for cloud effects.

After the simulation was completed, statistical measures of surface variables for the entire analysis domain were examined. Point-specific performance using time-series data was also examined. Overall, for the entire year, MM5 performed reasonably well. It did a good job in replicating the mean flow on a cell-to-cell basis. However, the 36-km resolution used in this modeling was clearly insufficient to resolve the complicated orographically-induced flows near the surface over the mountain regions in the western US. The wind fields aloft were modeled well everywhere. The surface moisture fields were modeled exceptionally well. Major synoptic features were captured, and only a couple of errors stood out (Olerud et al., 1999).

Finally, because most meteorological models (including MM5) are not designed specifically for air quality modeling purposes, a Meteorology-Chemistry Interface Processor (MCIP) was developed to address many issues related to data format translation, conversion of units of parameters, diagnostic estimations of parameters not provided, extraction of data for appropriate window domains, reconstruction of meteorological data on different horizontal and vertical grid resolutions through interpolation as needed, and to enforce consistency among the meteorological variables (Byun, 1999a, 1999b). The MCIP provides a complete set of meteorological data needed for the AQM simulations.

4. Results for regional modeling studies

Chemistry-transport simulations were performed using the CMAQ Chemical Tracer Model for calendar year 1996. The model domain consisted of a 36-km grid using 85×95 cells that extended 3060 km from California to Illinois and 3420 km from Mexico to Canada (Fig. 3). The results for O_3 and N deposition presented here are for a subdomain consisting of 29×26 grid cells centered over the Sierra Nevada.

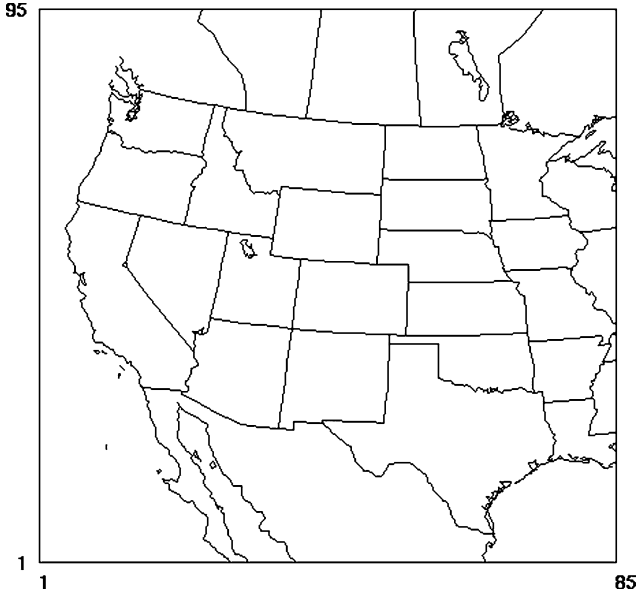

Figure 3. Model domain for the annual Community Multiscale Air Quality (CMAQ) regional haze modeling study using a 36-km grid with 85×95 grid cells.

The simulations were performed on inexpensive Linux based workstations using Athlon 1.566 gigahertz (GHz) central processing units (CPUs). The computational cost was 2 CPU hours per 24 hour simulation, or approximately 30 days of CPU time to simulate one calendar year. Output data storage requirements were approximately 1.5 GB per day, or 540 GB for the full year. Model evaluation was performed by comparing model predictions to ambient data for the IMPROVE network for aerosol species and to the Aerometric Information Retrieval Systems (AIRS) for ambient O_3 and NO_x data. (The model to data comparison are not described here but are available at the project Web site (http://path.cert.ucr.edu/rmc) and have been described by Tonnesen et al. (2002) and Wang et al. (2002).)

Figs. 4–6 show cumulative deposition of O_3, NO_2, HNO_3, NO_3^-, NH_3, and NH_4 for 1-month totals during January and July, 1996, for the southwestern US model subdomain. (Note that the dates listed within the figures are February 1 and August 1 which represents the end of the integration period for the months of January and July, respectively.) Although annual results are also available, the January and July results are used here to contrast the seasonal variations. In Fig. 4, the O_3 deposition flux reflects the product of the O_3 concentration and the deposition velocity. Areas of the domain with high O_3 deposition fluxes are associated with areas that tend to have high O_3 concentrations, e.g., the

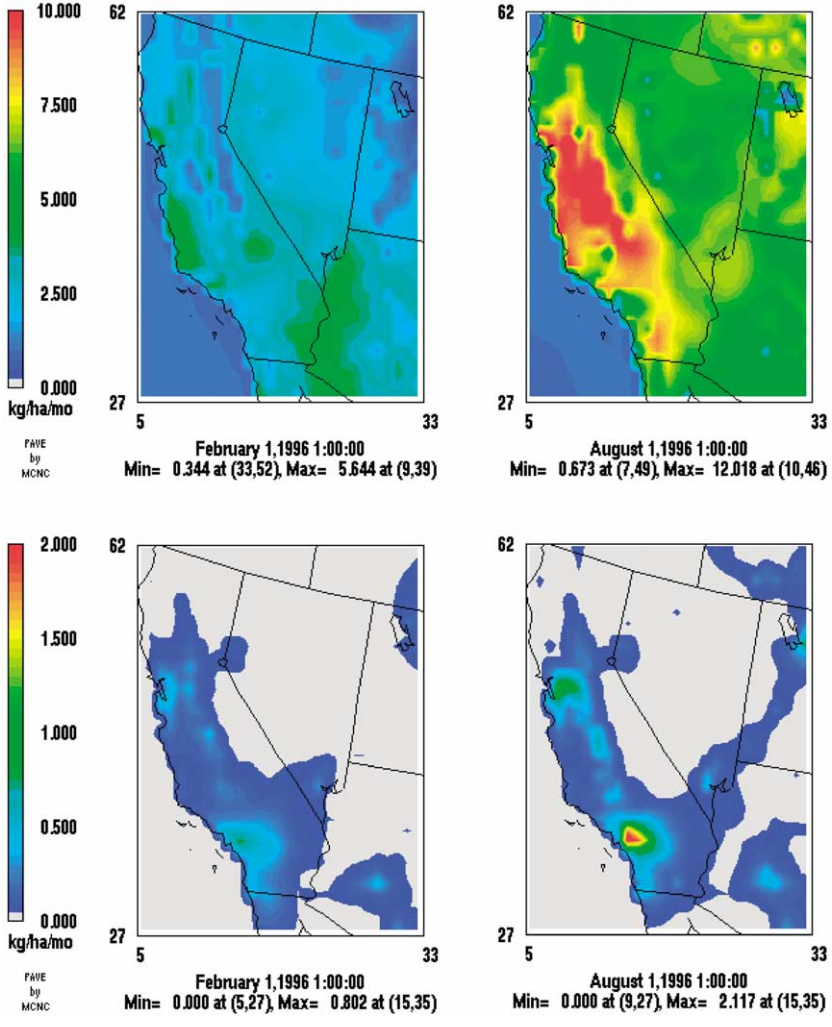

Figure 4. Cumulative O_3 deposition for January (top-left) and for July (top-right), and cumulative deposition of NO_2 for January (bottom-left) and July (bottom-right) 1996, for the southwestern US model subdomain. For all plots units are kg ha^{-1} month^{-1} and represent the totals for both wet and dry deposition.

central San Joaquin Valley (Fig. 4). The model simulations under-predicted O_3 concentrations for southern California, and this is reflected in the lower than expected deposition fluxes in southern California. The model performed well for O_3 in central and northern California, and Fig. 4 shows high rates

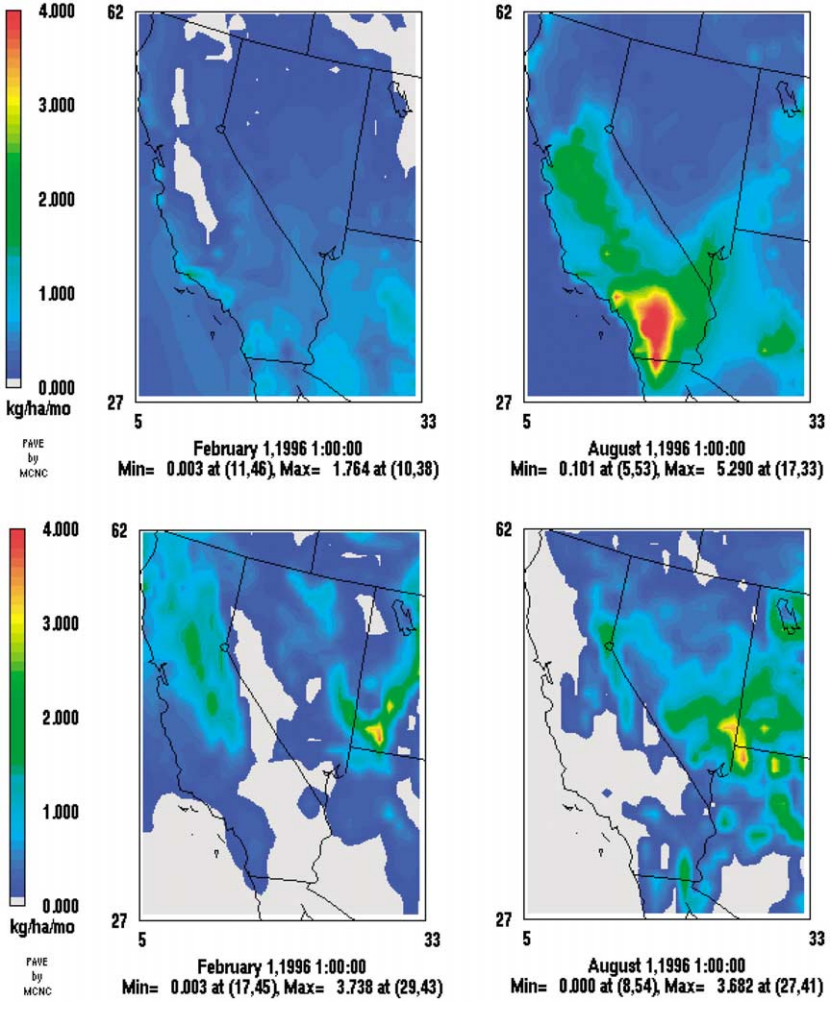

Figure 5. Cumulative HNO_3 deposition for January (top-left) and for July (top-right), and cumulative deposition of aerosol NO_3^- for January (bottom-left) and July (bottom-right) 1996, for the southwestern US model subdomain. For all plots units are $kg\,ha^{-1}\,month^{-1}$ and represent the totals for both wet and dry deposition.

of O_3 deposition in these areas with as much as 12 $kg\,ha^{-1}\,month^{-1}$ in July. There were substantially lower rates of O_3 deposition in the winter because there is reduced photochemical production of O_3 during this season, and this results in lower ambient O_3 concentrations. In addition, change in winter land

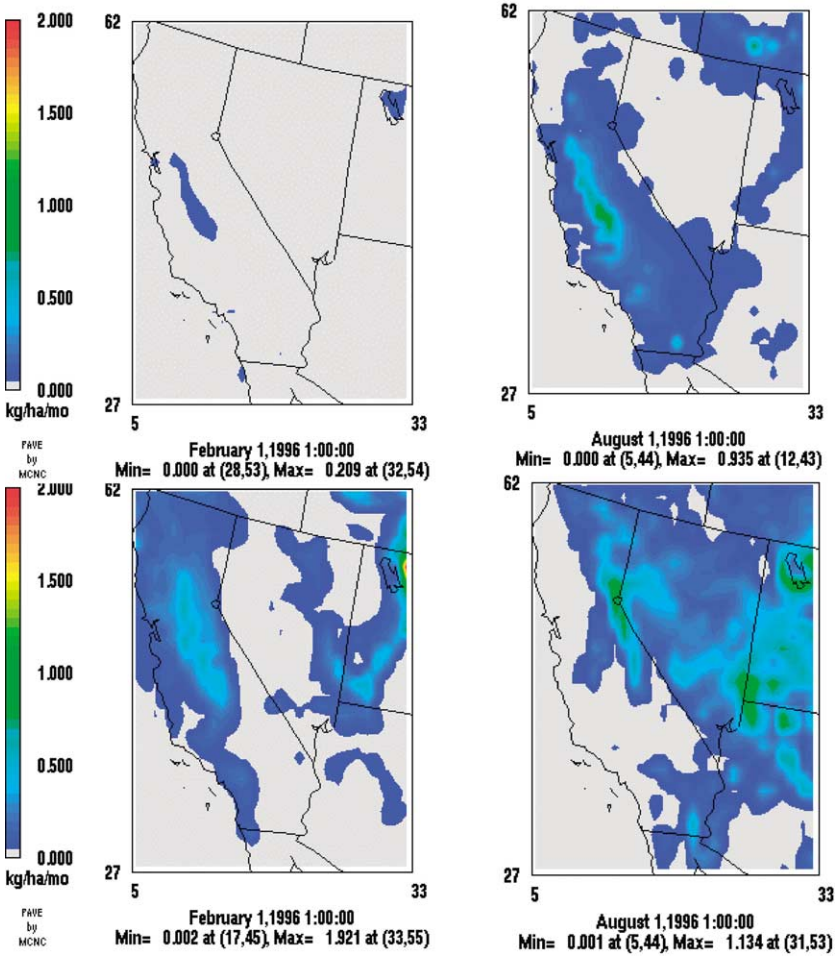

Figure 6. Cumulative NH_3 deposition for January (top-left) and for July (top-right), and cumulative deposition of aerosol NH_4^+ for January (bottom-left) and July (bottom-right) 1996, for the southwestern US model subdomain. For all plots units are $kg\,ha^{-1}\,month^{-1}$ and represent the totals for both wet and dry deposition.

use characteristics, such as loss of deciduous leaves, also tend to reduce the winter deposition velocity.

Fig. 4 also shows cumulative NO_2 deposition rates for January and July. Because NO_2 is short-lived, deposition of NO_2 is concentrated near the urban source regions. Deposition is highest near Los Angeles in the summer with a maximum of 2 $kg\,ha^{-1}\,month^{-1}$. There is also a large area with deposition

rates of between 0.1 to 0.3 kg ha^{-1} month^{-1} throughout large areas of California, but very low deposition rates of NO_2 in the Sierra Nevada.

Fig. 5 shows deposition rates of gas phase HNO_3 and of aerosol phase NO_3^-. Deposition of HNO_3 is low during January, especially in the Central Valley, whereas NO_3^- deposition is as large as 2 kg ha^{-1} month^{-1} for regions in the Central Valley and in the Sierra Nevada (Fig. 5). Because there are large emissions of NH_3 in the Central Valley and HNO_3 reacts with NH_3 to form nitrates for these conditions, the model predicted HNO_3 concentration is quite low. By contrast, for July high HNO_3 deposition rates were modeled throughout most of central and southern California with a peak rate of over 5 kg ha^{-1} mo^{-1}. Fig. 5 (bottom-right) shows surprising low deposition NO_3^- rates for July given that the model has high NH_3 emissions in the summer. A possible explanation is that transport through California is fast relative to deposition rate of NO_3^-. Alternative hypotheses are that the model underestimates the NH_3 emissions inventory, or that NH_3 reacts preferentially with sulfates in the summer months. Relatively high NO_3^- deposition rates were also modeled in the Sierra Nevada compared with other regions in California (Fig. 5).

Fig. 6 shows deposition rates of gas phase NH_3 and of aerosol phase NH_4^+. Deposition of gas phase NH_3 is nearly zero in the winter (Fig. 6), which may be a result of low NH_3 emissions and excess SO_4^{2-} and NO_3^- so that all available NH_3 rapidly converts to the aerosol phase. The cumulative deposition of aerosol NH_4^+ data for January supports this explanation because it shows substantial NH_4^+ deposition in the Central Valley in the winter. Fig. 6 shows substantial deposition of NH_3 in the Central Valley in the summer, and deposition of NH_4^+ in the summer is mostly in the Sierra Nevada. Presumably this is due to rapid transport of fine aerosols by westerly winds in the summer. The deposition of NH_3 and NH_4^+ in southern California appears surprisingly small given the large NH_3 sources in this region. It is very likely that there are substantial errors in the NH_3 inventory because aspect of the inventory is poorly known, there is high uncertainty in the emissions factors, and little effort has been made in developing necessary land use data for the purpose of NH_3 emissions estimates in this study.

Finally, Fig. 7 shows the summed N deposition as $NO_2 + HNO_3 + NO_3^- + NH_3 + NH_4^+$ for winter and summer conditions. The seasonal variability in N deposition is large, but seasonal variability in NO_x emissions is small. Although there is some seasonal variability in NH_3 emissions, it is unlikely to explain the differences shown in Fig. 7. A possible explanation is that NO emissions have a much longer lifetime in the wintertime and do not deposit within the domain shown here. For the summer condition, NO is rapidly converted to NO_2, HNO_3, and NO_3^- and these species have much larger deposition rates than NO. Depending on the lifetime of N for winter conditions, we might have expected to see N deposition shifted downwind to Nevada or Ari-

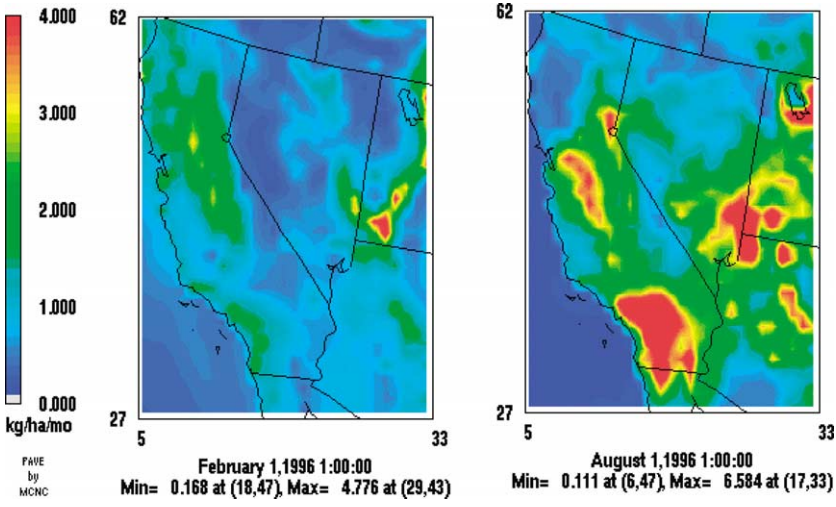

Figure 7. Total cumulative N deposition for January (left) and for July (right) 1996, for the southwestern US model subdomain, where $N = NO_2 + HNO_3 + NO_3^- + NH_3 + NH_4^+$. For all plots units are kg ha^{-1} month^{-1} and represent the totals for both wet and dry deposition.

zona. Our results show that this does not appear to be the case (Fig. 7), and this would imply that N is being transported on a continental or hemispheric scale for winter months. A more careful budget analysis of N species will be required to test these hypotheses.

Although these results are monthly totals, the model also predicts the hourly deposition rates, and these data may be useful for studying damage thresholds for vegetation. However, the current version of the model provides the average deposition flux for all vegetation types within a given grid cell. Future versions of the model will differentiate the deposition to different vegetation types within a grid cell, and this will provide more accurate estimates for damage assessments.

5. Conclusions and future work

The results of this study represent the first seasonal and annual budget analyses of N species using a detailed, comprehensive AQM. The interpretation of these results is difficult because of large uncertainties in the model inputs, especially the emissions inventories that are key to performing budget analyses. The uncertainties are largest for NH_3, which plays a central role in the conversion of HNO_3 to aerosols. Errors in the NO_x or VOC emissions may be responsible for model under-predictions of O_3 in southern California, and this in turn would

affect the rate of conversion of NO_x to HNO_3 and aerosol NO_3^-. Considerable effort will be required to develop improved emissions inventories for all model species, and this remains the highest priority for future work.

The photochemical reactions that control the production of O_3 and HNO_3 and the conversion of HNO_3 and NH_3 to aerosol nitrates are highly nonlinear in their dependence on species concentrations. Moreover, the 36 km grid does not adequately resolve orographic features in the Sierra Nevada. Therefore, the coarse model grid resolution using 36-km grid cells does not provide adequate spatial resolution. Eulerian AQMs with fine spatial resolution must be used to simulate the sources, transformation, and fate of these species for a wide range of seasonal and meteorological conditions. The results of our study represent a first attempt to perform long-term regional modeling using a relatively coarse grid resolution of 36-km by 36-km grid cells. Future work will use refined grids with resolutions of 12 km and 4 km.

Ambient monitoring data for evaluating or validating the model simulations are limited, and collection of more ambient data is essential. Previous applications of air quality models have focused primarily on short episodes of a few days or weeks, and ambient monitoring has mostly been designed to measure species concentrations with hourly or daily resolution to capture peak concentrations for episodic events. For evaluation of annual modeling used in budget analyses, a more useful approach would be longer-term monitoring with measurements integrated over periods of days or weeks. It will also be necessary to conduct special studies to examine the importance of orographic features (mountain tops versus valley) effects on pollutant concentrations.

Because the current effort is motivated by the study of regional haze, it is unlikely that this effort will address or resolve issues that are of concern to ecologists and wildland managers. However, if AQM studies are properly designed for wildland management, they hold the promise of providing data that cannot be achieved by other means, for example, providing estimates of O_3 and N deposition in regions with limited monitoring data. Modeling can also provide explanations for measurements and can evaluate the effect of alternate scenarios for management of O_3 and N deposition. The results presented in this chapter should be considered illustrative of the uses of air quality models, and considerable more effort and interaction among air quality modelers and ecologists will be required to realize the full potential of air quality modeling for wildland management.

Acknowledgments

This work has been supported by funding from the Western Governors' Association through the Western Regional Air Partnership (WRAP) modeling forum. The authors wish to acknowledge the contributions of other team members

who have participated in this project, especially staff at MCNC, ENVIRON Corporation, and the National Park Service. We thank Robin Dennis of the National Atmospheric and Oceanic Administration and also at the USEPA Atmospheric Modeling Division for helpful suggestions and comments on the manuscript.

References

Atkinson, R., 2000. Atmospheric chemistry of VOCs and NO_x. Atmos. Environ. 35, 2063–2101.

Binkowski, F., Shankar, U., 1995. The regional particulate matter model: Model description and preliminary results. J. Geophys. Res. 100, 26191–26209.

Binkowski, F., 1999. Aerosols in Models-3 CMAQ. In: Byun, D., Ching, J. (Eds.), Science Algorithms of the EPA Models-3 Community Multiscale Air Quality (CMAQ) Modeling System. EPA Tech. Rep. EPA-600/R-99/030.

Bytnerowicz, A., Padgett, P., Percy, K., Krywult, M., Riechers, G., Hom, J., 1999. Direct effects of nitric acid on forest trees. In: Miller, P.R., McBride, J.R. (Eds.), Oxidant Air Pollution Impacts in the Montane Forests of Southern California. In: Ecological Series, Vol. 134. Springer, pp. 270–287.

Byun, D., Ching, J. (Eds.), 1999. Science Algorithms of the EPA Models-3 Community Multiscale Air Quality (CMAQ) Modeling System. EPA Tech. Rep. EPA-600/R-99/030. Available from EPA/ORD, Washington, DC, p. 20460.

Byun, D., 1999a. Dynamically consistent formulations in meteorological and air quality models. Part I: Governing equations in a generalized coordinate system. J. Atmos. Sci. 56, 3787–3807.

Byun, D., 1999b. Dynamically consistent formulations in meteorological and air quality models. Part II: Mass conservation issues. J. Atmos. Sci. 56, 3808–3820.

CARB, 2000. Methodology for estimating emission from on-road motor vehicles. California Air Resources Board, California Environmental Protection Agency, Sacramento.

Chang, J.S., Brost, R.A., Isaksen, I.S.A., Middleton, P., Stockwell, W.R., Walcek, C.J., 1987. A three-dimensional Eulerian Acid Deposition model: Physical concepts and formulation. J. Geophys. Res. 92 (14), 681–700.

Christoforou, C.S., Salmon, L.G., Hannigan, M.P., Solomon, P.A., Cass, G.R., 2000. Trends in fine particle concentration and chemical composition in Southern California. J. Air Waste Manag. Assoc. 50, 43–53.

Colela, P., Woodward, P.R., 1984. The piecewise parabolic method (PPM) for gas-dynamical simulations. J. Comput. Phys. 54, 174–201.

Daum, P.H., Kleinman, L., Imre, D.G., Nunnermacker, L.J., Lee, Y.-N., Springston, S.R., Newman, L., 2000. Analysis of the processing of Nashville urban emissions on July 3 and July 18, 1995. J. Geophys. Res. 105, 9155–9164.

Dennis, R.L., Mchenry, J.N., Barchet, W.R., Binkowski, F.S., Byun, D.W., 1993. Correcting RADM's sulfate underprediction: Discovery and correction of model errors and testing the corrections through comparisons against field data. Atmos. Environ. 26A, 975–997.

Dodge, M.C., 2000. Chemical oxidant mechanisms for air quality modeling: critical review. Atmos. Environ. 34, 2103–2130.

ENVIRON, 1998. User's Guide Comprehensive Air Quality Model with Extensions (CAMx) Version 2.00. ENVIRON Corporation, Novato, CA.

Finlayson-Pitts, B.J., Pitts Jr., J.N., 1986. Atmospheric Chemistry: Fundamentals and Experimental Techniques. John Wiley and Sons, New York, NY.

Gao, S., Hegg, D.A., Frick, G., Caffrey, P.F., Pasternack, L., Cantrell, C., Sullivan, W., Ambrusko, J., Albrechcinski, T., Kirchstetter, T.W., 2001. Experimental and modeling studies of secondary

organic aerosol formation and some applications to the marine boundary layer. J. Geophys. Res. 106, 27619–27634.

Gery, M.W., Whitten, G.Z., Killus, J.P., Dodge, M.C., 1989. A photochemical kinetics mechanism for urban and regional scale photochemical modeling. J. Geophys. Res. 94, 12925–12956.

Gillani, N.V., Pleim, J.E., 1996. Subgrid scale features of anthropgenic emissions of VOC and NO_x in the context of regional Eulerian models. Atmos. Environ. 30, 2043–2059.

Grell, A.G., Dudhia, J., Stauffer, D.R., 1994. A description of the fifth-generation Penn State/NCAR mesoscale model (MM5). NCAR Tech. Note NCAR/TN-398+STR, National Center for Atmospheric Research, Boulder, CO.

Hertel, O., Berkowicz, R., Christensen, J., Hov, O., 1993. Test of two numerical schemes for use in atmospheric transport-chemistry models. Atmos. Environ. 27A, 2591–2611.

Houyoux, M.R., Vukovich, J.M., Coats, C.J. Jr., Wheeler, N.J.M., Kasibhatla, P.S., 2000. Fast emissions modeling with the sparse matrix operator kernel emissions modeling system. J. Geophys. Res. 105, 9079–9090.

Hughes, L.S., Allen, J.O., Kleeman, M.J., Johnson, R.J., Cass, G.R., Gross, D.S., Gard, E.E., Galli, M.E., Morrical, B.D., Fergenson, D.P., Dienes, T., Noble, C.A., Silva, P.J., Prather, K.A., 1999. Size and composition distribution of atmospheric particles in Southern California. Environ. Sci. Tech. 33, 3506–3515.

ICF, 2002. User's Guide to the Regional Modeling System for Aerosols and Deposition (REMSAD) Version 6. ICF Consulting, March 29, 2002. Available at: http://remsad.saintl.com/documents/remsad_users_guide_final_03-29-02.doc.

Jeffries, H.E., Tonnesen, G.S., 1994. Comparison of two photochemical reaction mechanisms using a mass balance and process analysis. Atmos. Environ. 28, 2991–3003.

Kavouras, I.G., Mihalopoulos, N., Stephanou, E.G., 1999. Secondary organic aerosol formation vs primary organic aerosol emission: In situ evidence for the chemical coupling between monoterpene acidic photooxidation products and new particle formation over forests. Environ. Sci. Tech. 33, 1028–1037.

Kleindienst, T.E., Smith, D.F., Li, W., Edney, E.O., Driscoll, D.J., Speer, R.E., Weathers, W.S., 1999. Secondary organic aerosol formation from the oxidation of aromatic hydrocarbons in the presence of dry submicron ammonium sulfate aerosol. Atmos. Environ. 33, 3669–3681.

Kleinman, L.I., 1994. Low- and high-NO_x tropospheric photochemistry. J. Geophys. Res. 99 (16), 831–838.

Kleinman, L.I., Daum, P.H., Imre, D.G., Lee, J.H., Lee, Y.-N., Nunnermacker, L.J., Springston, S.R., Weinstein-Lloyd, J., Newman, L., 2000. Ozone production in the New York City urban plume. J. Geophys. Res. 105 (14), 495–511.

Lamb, R.G., 1983. A regional scale (100 km) model of photochemical air pollution. Part 1: theoretical foundation. Technical Report EPA-6000/3-83-035, Environmental Protection Agency, Washington, DC.

Malm, W.C., 2000. Spatial and seasonal patterns and temporal variability of haze and its constituent components in the United States. May, 2000. Cooperative Institute for Research in the Atmosphere, Colorado State University, Fort Collins, CO 80253.

McRae, G.J., Goodin, W.R., Seinfeld, J.H., 1982. Development of a second-generation mathematical model for urban air pollution: model formulation. Atmos. Environ. 16, 679–696.

McRae, G.J., Russell, A.G., 1984. Dry deposition of nitrogen-containing species. In: Hicks, B.B. (Ed.), Deposition Both Wet and Dry. In: Teasley, J.I. (Ed.), Acid Precipitation Series. Butterworth Publishers Stoneham, MA. Chapter 9, pp. 153–194.

NAPAP, 1991. National Acid Precipitation Assessment Program: 1990 integrated assessment report. National Acid Precipitation Assessment Program, Washington, DC.

National Research Council, 1992. Rethinking the Ozone Problem in Urban and Regional Air Pollution. National Academy Press, Washington, DC.

National Research Council, 1993. Protecting Visibility in National Parks and Wilderness Areas. National Academy Press, Washington, DC.

Olerud, D., Alapaty, K., Wheeler, N., 1999. Meteorological modeling of 1996 for the United States with MM5. Final Report submitted to the Office of Air Quality Planning Standards, Durham, NC 27711. EPA Task Order Number CAA689805.

Pierce, T., Geron, C., Bender, L., Dennis, R.L., Tonnesen, G.S., Guenther, A., 1998. Influence of isoprene emissions on regional ozone modeling. J. Geophys. Res. 103, 25611–25629.

Reich, P.B., Amundson, R.G., 1985. Ambient levels of ozone reduce net photosynthesis in trees and crop species. Science 230, 566–570.

Roselle, S.J., Binkowski, F.S., 1999. Cloud dynamics and chemistry. In: Byun, D., Ching, J. (Eds.), Science algorithms of the EPA models-3 Community Multiscale Air Quality (CMAQ) Modeling System. EPA Tech. Rep. EPA-600/R-99/030.

Russell, A., Dennis, R., 2000. NARSTO critical review of photochemical models and modeling. Atmos. Environ. 34, 2283–2324.

Seaman, N.L., 1999. Meteorological modeling for air-quality assessments. Atmos. Environ. 34, 2231–2259.

Seinfeld, J.H., Pandis, S.N., 1998. Atmospheric Chemistry and Physics. John Wiley and Sons, New York, NY.

Sillman, S., 1995. The use of NO_y, H_2O_2, and HNO_3 as indicators for ozone-NO_x-hydrocarbon sensitivity in urban locations. J. Geophys. Res. 100, 14175–14188.

Simpson, D., 1992. Long period modeling of photochemical oxidants in Europe: calculations for July 1985. Atmos. Environ. 26, 1609–1634.

Strader, R., Lurmann, F., Pandis, S.N., 1999. Evaluation of secondary organic aerosol formation in winter. Atmos. Environ. 33, 4849–4863.

Tonnesen, G.S., Jeffries, H.E., 1994. Inhibition of odd oxygen production in the carbon bond four and the generic reaction set mechanisms. Atmos. Environ. 28, 1339–1349.

Tonnesen, G.S., Wang, Z.S., Omary, M., Chien, C.J., Wang, B., 2002. Regional aerosol and visibility modeling using the Community Multiscale Air Quality Model for the western US: Results and model evaluation for the 1996 annual simulation. In: WESTAR Technical Conference On Regional Haze Modeling, February 12–14, 2002, Riverside, CA.

USEPA, 1996. Air Quality Criteria for Ozone and Related Photochemical Oxidants. Vol. II. EPA/600/P-93/004bF.

USEPA, 1997a. 62 Federal Register 38652.

USEPA, 1997b. Deposition of Air Pollutants to the Great Waters: Second Report to Congress. US Environmental Protection Agency Office of Air Quality Planning and Standards, Durham, NC 27711.

Valigura, R.A., Alexander, R.B., Castro, M.S., Meyers, T.P., Paerl, H.W., Stacey, P.E., Turner, R.U., 2001. Nitrogen Loading in Coastal Water Bodies: An Atmospheric Perspective. In: Coastal and Estuarine Studies, Vol. 57. American Geophysical Union, Washington, DC.

Vitousek, P.M., Aber, J.D., Howarth, R.W., Likens, G.E., Matson, P.A., Schindler, D.W., Schlesinger, W.H., Tilman, D.G., 1997. Human Alteration of the Global Nitrogen Cycle: Causes and Consequences. Ecological Applications 7, 737–750.

Wang, Z.S., Tonnesen, G.S., Omary, M., Chien, C.J., Wang, B., 2002. Model intercomparison for regional aerosol and visibility using the CMAQ and REMSAD air quality models. In: WESTAR Technical Conference On Regional Haze Modeling, February 12–14, 2002, Riverside, CA.

Wesley, M.L., 1989. Parameterization of surface resistance to gaseous resistance to dry deposition in regional-scale numerical models. Atmos. Environ. 23, 1293–1304.

Whitby, K.T., 1978. The physical characteristics of sulfur aerosols. Atmos. Environ. 12, 135–159.

Wilkins, E.T., 1954. Air pollution and the London fog of 1952. J. R. Sanitary Inst. 74, 1–12.